

Supplementary Information

A facilely-synthesized polyanionic cathode with impressive long-term cycling stability for sodium-ion batteries

Jie Li,^{a,b} Yuruo Qi,^{*a,b} Fangyuan Xiao,^{a,b} Shu-Juan Bao,^{a,b} and Maowen Xu^{*a,b}

^a Key Laboratory of Luminescence Analysis and Molecular Sensing (Southwest University), Ministry of Education, School of Materials and Energy, Southwest University, Chongqing 400715, PR China

^b Chongqing Key Lab for Advanced Materials and Clean Energies of Technologies, Southwest University, Chongqing 400715, PR China.

E-mail: qiyurujy@swu.edu.cn; xumaowen@swu.edu.cn

Experimental section

Materials synthesis

All the chemical reagents were purchased and used without any further purification. NH_4VO_3 (analytical reagent (AR) grade), NaI (AR grade) and H_3PO_4 (≥ 85 wt.% in H_2O) were purchased from Aladdin Industrial Corporation.

$\text{Na}_{0.5}\text{VOPO}_4 \cdot 2\text{H}_2\text{O}$ was prepared by a simple chemical precipitation method at room temperature. Firstly, 5 mmol NaI and 20 mL ethanol were added into 10 mL deionized water to prepare solution A. 2 mmol NH_4VO_3 and 0.5 mL H_3PO_4 were added into 30 mL deionized water with magnetic stirring to prepare solution B. Then, solution B was drop-by-drop added to solution A. The mixture was stirred for 5 h at room temperature. The product was dried at 60 °C after filtration and washing with deionized water and ethanol.

Materials characterization

The morphology of the samples was observed by field emission scanning electron microscopy (FESEM, JSM-7800F, Japan). Transmission electron microscope (TEM) images were acquired using a JEM-2100F. The thickness of the NVOP nanosheets was determined by an atomic force microscope (AFM, Bruker-Icon SPM). XRD patterns were measured using Cu K_α radiation (1.5418 Å) on an X-ray diffractometer (Bruker, Advance D8A A25) from 5° to 80° (2 θ). X-ray photoelectron spectroscopy (XPS) measurements were conducted by Thermo Scientific ESCALAB 250Xi electron spectrometer. The atomic ratio of Na/V in the as-synthesized product was characterized by Inductively Coupled Plasma Optical Emission Spectrometer (ICP-OES, PerkinElmer Optima 8000).

The water content was analyzed by thermogravimetric analysis (TGA, Q50, USA) under N₂ atmosphere with a heating rate of 10 °C min⁻¹.

Electrochemical measurements

The as-synthesized product was used as cathode active material for SIBs. The active material, Ketjen Black and sodium carboxymethyl cellulose (CMC) binder were mixed in a weight ratio of 7:2:1 with deionized water. The slurry was coated on aluminum foils and dried at 60 °C for 12 h. The mass loading of active materials is about 2 mg cm⁻². To measure the electrochemical performance, coin-type (CR2032) cells were assembled in an argon-filled glove box. The electrolyte was 1 M NaClO₄ with 5% fluoroethylene carbonate (FEC) in ethylene carbonate (EC)/Diethyl carbonate (DEC) (1:1 in volume). The amount of electrolyte solution added in each cell was 45 μL. The counter electrodes were pure sodium foils and the separators were Celgard 2400 separators. All the charge and discharge measurements were conducted on a Land BT2000 battery test system (Wuhan, China) under room temperature while the cut-off voltage was maintained between 2.0 and 4.5 V. The cyclic voltammetry (CV) test was carried out on a CHI 660e electrochemical workstation at different scan rates of 0.1, 0.2, 0.3, 0.4, 0.5 mV s⁻¹. The apparent diffusion coefficient can be calculated from the slope of fitting lines via the Randles-Sevcik equation:

$$i_p = (2.69 \times 10^5) n^{\frac{3}{2}} A D^{\frac{1}{2}} C v^{\frac{1}{2}}$$

Where i_p is the current at an electrochemical reaction (A), n is the number of electrons participating in one mole of the reaction, A is the electrode-electrolyte interface

area (approximately to be the electrode area, 1.327 cm^2), D is the apparent diffusion coefficient ($\text{cm}^2 \text{ s}^{-1}$), C is the mole concentration of Na^+ in the electrode (mol cm^{-3}), and ν is the scan rate (V s^{-1}).

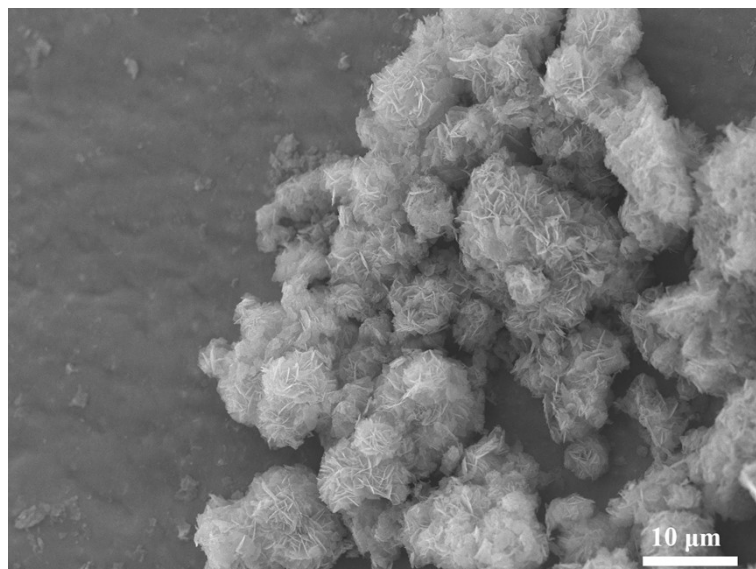


Fig. S1. FESEM image of NVOP.

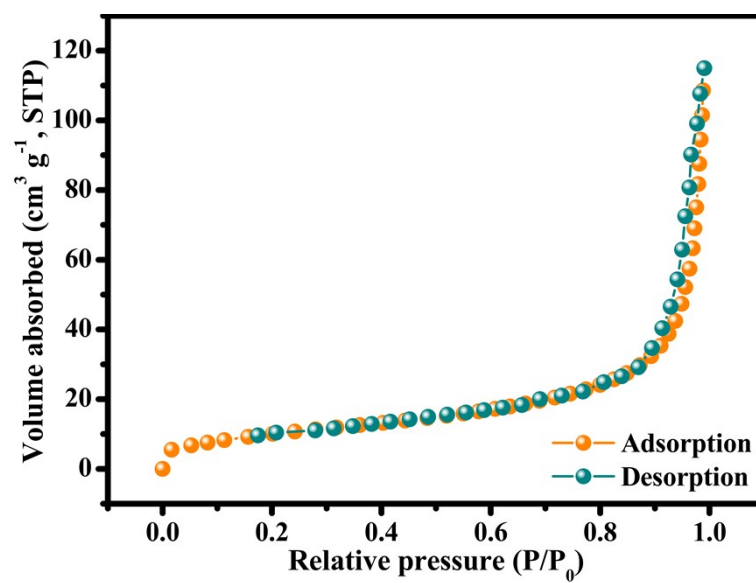


Fig. S2. Nitrogen adsorption-desorption isotherms of NVOP.

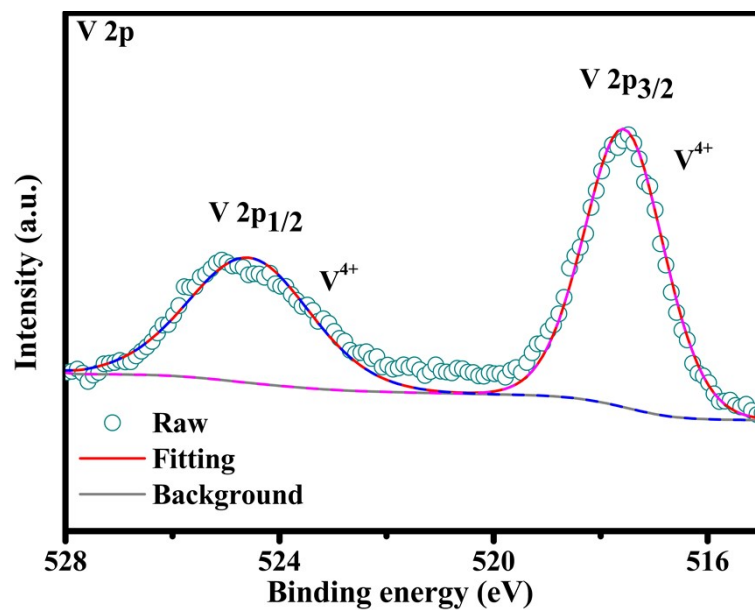


Fig. S3. High-resolution V 2p XPS spectrum of the NVOP electrode discharge to 2.0 V.

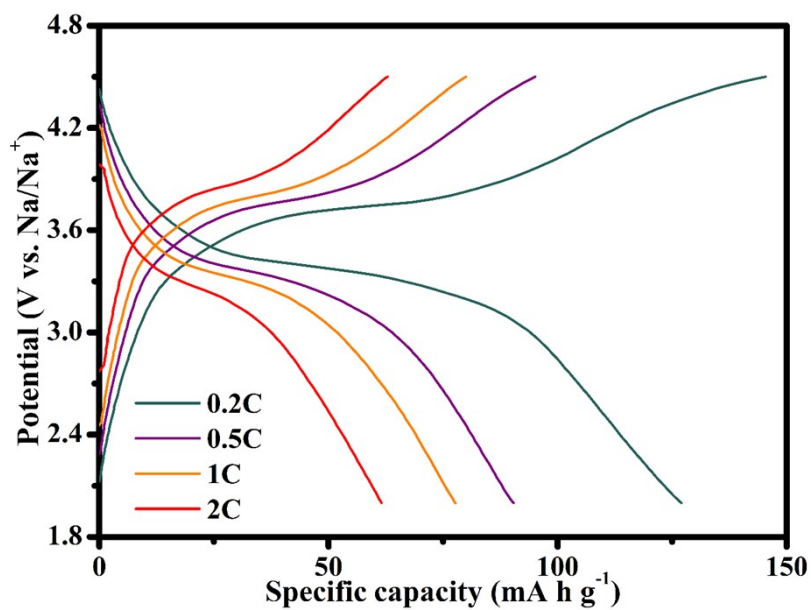


Fig. S4. The galvanostatic charge/discharge profiles of the NVOP electrode at various current densities.

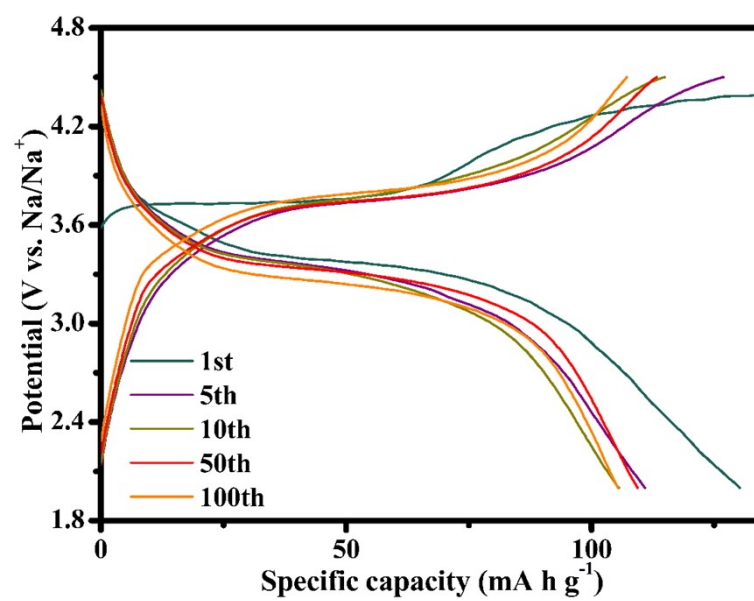


Fig. S5. Galvanostatic charge/discharge profiles of the NVOP electrode at 0.2C.

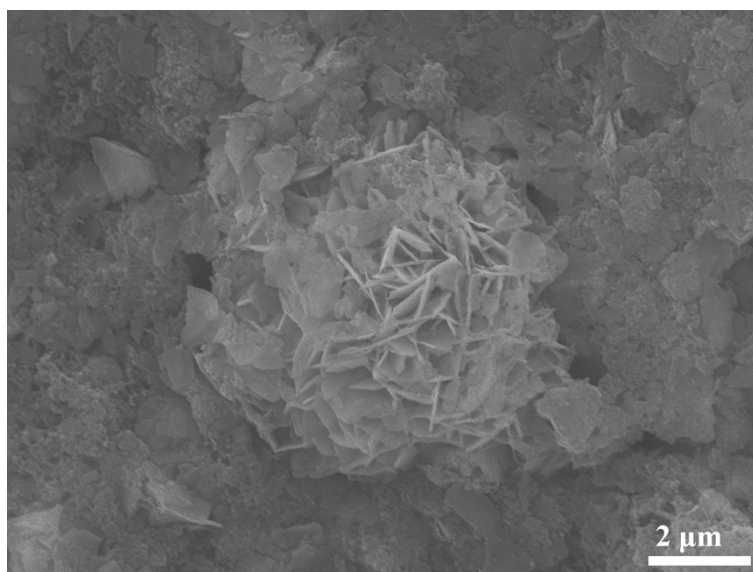


Fig. S6. FESEM image of the NVOP electrode after 60 cycles at 1C.

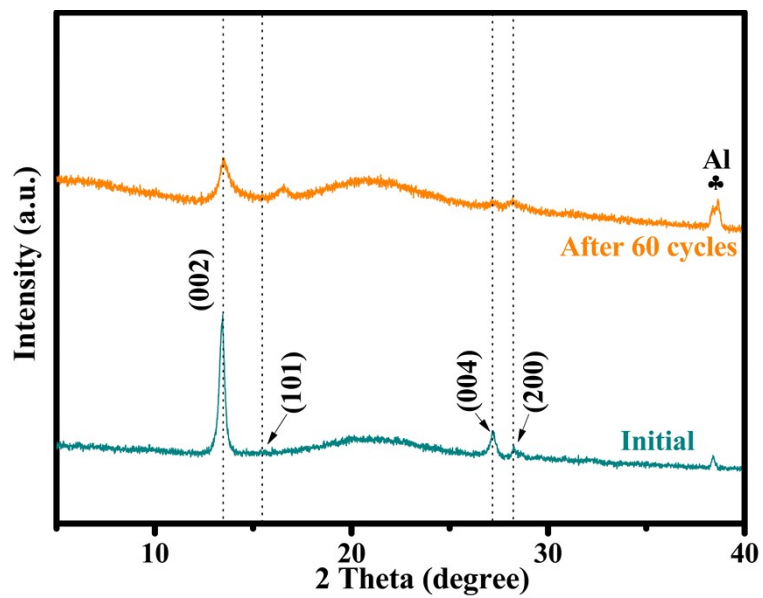


Fig. S7. XRD patterns of the NVOP electrode before and after 60 cycles at 1C.

Table S1. XRD powder diffraction and Rietveld-refined results of the as-prepared NVOP.

Symmetry	Triclinic			
Space group	<i>P</i> -1			
Lattice parameters	$a = 6.462 \text{ \AA}$	$b = 6.457 \text{ \AA}$	$c = 13.693 \text{ \AA}$	$V = 561.529 \text{ \AA}^3$
	$\alpha = 87.375^\circ$	$\beta = 79.678^\circ$	$\gamma = 89.972^\circ$	
Rwp	4.97%			
Rp	3.33%			
Rexp	0.215%			
GOF	5.842			

	M_1 (mg/L)	M_2 (mg/L)	M_3 (mg/L)	The average molar ratio of Na/V	Table S2.
Na	1.162	1.193	1.183	0.5094:1	Results of
V	5.174	5.054	5.161		ICP

analysis

of NVOP.

Table S3. Comparison of the apparent diffusion coefficients of sodium ion with typical polyanionic electrodes for SIBs.

Materials	Diffusion coefficient (cm ² s ⁻¹)	Reference
Na _{0.5} VOPO ₄ ·2H ₂ O	around 10 ⁻¹¹	This work
Na _{3+x} Mn _x V _{1-x} Cr(PO ₄) ₃	3.24 × 10 ⁻⁹ (x = 0)	1
	2.84 × 10 ⁻¹⁰ (x = 0.2)	
	1.86 × 10 ⁻¹⁰ (x = 0.4)	
	8.16 × 10 ⁻¹¹ (x = 0.6)	
	3.18 × 10 ⁻¹¹ (x = 0.8)	
	9.21 × 10 ⁻¹¹ (x = 1)	
Na ₃ V ₂ (PO ₄) ₂ F ₃ /rGO	around 10 ⁻¹² - 10 ⁻¹⁰	2
NaVPO ₄ F/C	around 10 ⁻¹¹	3
NaVOPO ₄	2 × 10 ⁻¹² - 1 × 10 ⁻¹¹	4
Na ₄ VO(PO ₄) ₂	5.1 × 10 ⁻¹¹	5
Na ₃ V ₂ (PO ₄) ₂ F ₃ /C	around 10 ⁻¹²	6
Na ₂ FePO ₄ F/C	3.63 × 10 ⁻¹²	7
Na ₂ FeSiO ₄ /C	2.53 × 10 ⁻¹³	8

References

- 1 R. Klee, P. Lavela and J. L. Tirado, *Electrochim. Acta*, 2021, **375**, 137982.
- 2 Y. Subramanian, W. Oh, W. Choi, H. Lee, M. Jeong, R. Thangavel and W. S. Yoon, *Chem. Eng. J.*, 2021, **403**, 126291.
- 3 C. Chen, T. Li, H. Tian, Y. Zou and J. Sun, *J. Mater. Chem. A*, 2019, **7**, 18451–18457.
- 4 C.-Y. Chen, K. Matsumoto, T. Nohira and R. Hagiwara, *J. Electrochem. Soc.*, 2015, **162**, A2093.
- 5 P. A. Aparicio and N. H. de Leeuw, *Phys. Chem. Chem. Phys.*, 2020, **22**, 6653–6659.
- 6 G. dong Yi, C. ling Fan, Z. Hu, W. hua Zhang, S. chang Han and J. shui Liu, *Electrochim. Acta*, 2021, **383**, 138370.
- 7 J. Zhang, X. Zhou, Y. Wang, J. Qian, F. Zhong, X. Feng, W. Chen, X. Ai, H. Yang and Y. Cao, *Small*, 2019, **15**, 1903723.
- 8 W. Guan, B. Pan, P. Zhou, J. Mi, D. Zhang, J. Xu and Y. Jiang, *ACS Appl. Mater. Interfaces*, 2017, **9**, 22369–22377.
- 9 J. Zhang, X. Zhao, Y. Song, Q. Li, Y. Liu, J. Chen and X. Xing, *Energy Storage Mater.*, 2019, **23**, 25–34.